Estimating the fractal dimension of plants using the two-surface method. An analysis based on 3D-digitized tree foliage.

Frédéric Boudon
INRIA-Lorraine
615, rue du Jardin Botanique
54600 Villers-lès-Nancy, France

Christophe Godin
INRIA-Sophia Antipolis,
UMR AMAP TA/40E
34398 Montpellier
Cedex 5, France

Christophe Pradal
CIRAD,
UMR AMAP TA/40E
34398 Montpellier
Cedex 5, France

Olivier Puech
INRA,
UMR AMAP TA/40E
34398 Montpellier
Cedex 5, France

Hervé Sinoquet
INRA-UBP, UMR PIAF
Domaine de Crouelle,
234, avenue du Brézet
63100 Clermont-Ferrand, France

Abstract

In this paper, we present a method to estimate the fractal dimension of plant foliage in 3-dimensions (3D). This method is derived from the two-surface method introduced in the 90's to estimate the fractal dimension of tree species from field measurements on collections of trees. Here we adapted the method to individual plants. The multiscale topology and geometry of the plant must first be digitized in 3D. Then leafy branching systems of different sizes are constructed from the plant database, using the topological information. 3D convex envelops are then computed for each leafy branching system. The fractal dimension of the plant is finally estimated by comparing the total leaf area and the convex envelop area of these leafy modules. The method was assessed on a set of 4 peach trees entirely digitized at shoot scale. Results show that the peach trees have a marked self-similar foliage with fractal dimension close to 2.4.

Keywords: Fractal dimension, two-surface method, box counting method, plant architecture, foliage distribution, multiscale analysis.

1 INTRODUCTION

Plant geometry is a key factor in the modeling of plant functioning and growth. It represents the exchange interface between internal physiological processes and the environment. This interaction may concern either the abiotic (resource capture, heat dissipation) or the biotic (disease propagation, insect movement) environment. Characterizing the geometry of plants is thus a challenging problem in the functional-structural modeling of plants [1].

Contrary to most handcrafted objects, the geometry of many natural objects is very irregular and presents intricate structures at different scales. This is particularly true for plants that may show, depending on the species, complex and irregular crown shapes or spatial distributions of leaves [2]. As illustrated in [3], fractal geometry [4] offers a useful framework to study the geometry of such irregular objects in biology.

A few studies have already been made in this direction to analyze the irregularity of plants by determining their supposed fractal dimension. This parameter is of major importance in the study of plant architecture since it characterizes the way plants physically penetrate into the 3D space. Most of these studies were carried out on woody structures, and especially on root systems using the classical box-counting method [5],[6],[7]. Only a few works have addressed the problem of determining the fractal dimension of plant foliage [8],[9]. However, none of these methods were applied on 3D foliage structures. Morse *et al.* for instance [8] used the box-counting method on plant foliage pictures to estimate the fractal dimension of real plants and used this result to explain different distributions of anthropods populations at different scales in the vegetation. A different method was introduced in [10],[11], where the fractal dimension of

forest tree species was estimated from estimation of leaf area and crown surface of individual trees. This two-surface method relies on the assumption that plants are self-similar organisms.

In this paper, we consider the problem of estimating the fractal dimension of an individual tree using a method derived from the two-surface method. We first review the theoretical aspects of the two-surface method and illustrate it on theoretical examples. We then present a multiscale model of plant geometry and show how this model can be used to compute plant envelops at different scales. These algorithms are then used to apply the two-surface method to 3D-digitized plant foliages (peach trees) and derive their individual fractal dimension.

2 THE TWO-SURFACE METHOD

The two-surface method [10] exploits a scaling property of fractal objects for estimating their fractal dimension. It is based on the idea that, through magnification or reduction, the relationship between the size of the envelop of an object (i.e. its diameter, surface or volume) and the measure at scale δ of its contents follow particular scaling rules that depend on the fractal dimension D of the object. This relationship links the fractal contents of an object to its non-fractal envelop. It is thus symmetrical to the length-area relationship discussed in [4] which links the measure of a non-fractal object with its fractal boundary [10].

Let us consider an object P and a unit of measurement of dimension D of size δ ($D = 1$ for a yardstick, $D = 2$ for a tile or $D = 3$ for a paving volume). We call $\mu_\delta^D(P)$ the *measure of P at scale δ*, obtained by tiling P with the paving units of size δ and dimension D, and by summing up the measures of these $N_\delta(P)$ tiles. By construction, $\mu_\delta^D(P)$ ignores details of size less than δ [12].

For many objects, including regular and fractal objects, the number of tiles $N_\delta(P)$ behaves as a power law as δ decreases to 0:

$$N_\delta(P) \propto \delta^{-d} \tag{1}$$

meaning that $N_\delta(P)$ gets proportional to δ^{-d} as δ tends to 0. The power value, d, can be identified with the dimension of the object [4]. Since all the tiles have the same elementary measure, δ^D, the measure $\mu_\delta^D(P)$ can thus be expressed as:

$$\mu_\delta^D(P) = N_\delta(P)\,\delta^D \propto \delta^{D-d}. \tag{2}$$

This expression shows that the measure of P at scale δ gets independent of the measurement unit δ when $D = d$, *i.e.* when the integer dimension of the paving unit matches the dimension of the object. In such a case, we shall simply note $\mu_\delta^D(P) = \mu^D(P)$.

For fractal objects of dimension d, this measure has the following important property. If the object P is dilated by a factor λ, its measure is multiplied by a factor λ^d [12]. This *scaling property* of fractal objects is at the origin of the two-surface method. It relies on the idea that the measure at scale δ of an object dilated by a factor λ is identical to the measure at scale $\frac{\delta}{\lambda}$ of the initial, non-dilated, object :

$$\mu_\delta^D(\lambda P) = N_\delta(\lambda P)\,\delta^D = N_{\frac{\delta}{\lambda}}(P)\,\delta^D \tag{3}$$

Hence,

$$\mu_\delta^D(\lambda P) \propto \left(\frac{\delta}{\lambda}\right)^{-d} \delta^D = \lambda^d \delta^{D-d} \tag{4}$$

which finally yields the scaling property:

$$\mu_\delta^D(\lambda P) = \lambda^d\,\mu_\delta^D(P). \tag{5}$$

Now, let us consider a regular object $\mathcal{E}(P)$, called the *extension* of P, characterizing the amount of space occupied by P. $\mathcal{E}(P)$ can be defined for instance as a diameter of P, *i.e.* a straight line segment between two given points of P whose size equals the maximum Euclidean distance between any two points of P, or as the minimal convex envelop containing P, *etc.* Being regular, $\mathcal{E}(P)$ has an integer dimension D'. Its measure $\mu^{D'}(\mathcal{E}(P))$ is thus independent of the measurement unit δ and verifies the scaling property :

$$\mu^{D'}(\lambda\,\mathcal{E}(P)) = \lambda^{D'}\mu^{D'}(\mathcal{E}(P)). \tag{6}$$

By eliminating λ between Eqs. 5 and 6 we get:

$$\mu_\delta^D(\lambda P) = \left(\frac{\mu^{D'}(\lambda \mathcal{E}(P))}{\mu^{D'}(\mathcal{E}(P))} \right)^{\frac{d}{D'}} \mu_\delta^D(P)$$

Denoting:

$$a = \frac{\mu_\delta^D(P)}{\mu^{D'}(\mathcal{E}(P))^{\frac{d}{D'}}}$$

we get the two-surface Eq.:

$$\mu_\delta^D(\lambda P) = a\, \mu^{D'}(\mathcal{E}(\lambda P))^{\frac{d}{D'}} \tag{7}$$

Equation (7) holds for any value of λ. The term a only depends on measures of the initial object P and its extension. It is independent of the dilation factor λ. Equation (7) expresses that the measure at scale δ of an object dilated by any factor λ, is proportional to the measure of the extension of the dilated object to the power d/D', d being the fractal dimension of P and D' the dimension of the paving unit. As noted by Zeide and Pfeifer [10], if both detailed surfaces at scale δ and extension surfaces can be measured or estimated for a family of fractal objects with varying sizes, this Eq. makes it possible to estimate the fractal dimension of this family by linear regression between the Log values of both surfaces.

Example 1. Let us first illustrate this property on a simple example. Consider the von Koch curve C illustrated in Fig. 1. To measure the extent of C at different dilation scales, we choose a unit of measurement δ of dimension $D = 1$ (δ is a yardstick) and we consider the following dilations of C: $C_0 = C, C_1 = 3C, C_2 = 9C$,..., $C_n = 3^n C$. At dilation scale 0 (Fig. 1.C_0), $\mu_\delta^1(C_0) = 2\delta = l_0$, the curve C_0 looks like a straight segment.

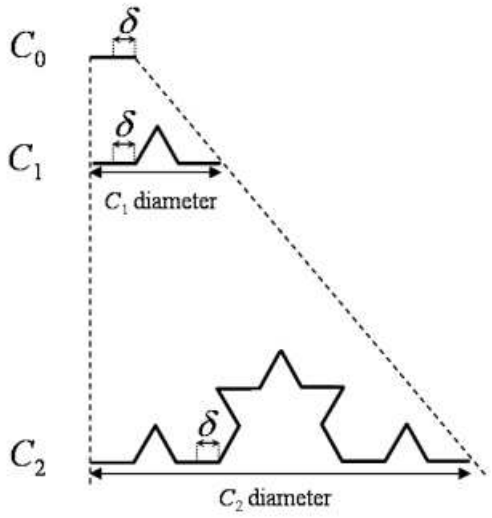

Figure 1. a series of dilated von Koch curves. Using a fixed measurement unit δ, the observer can see an increasing number of details with increasing dilation factors (from C_0 to C_2). However the increase rate of the number of details is different from the increase rate of the curve diameter: when the diameter is multiplied by 3, the number of details is multiplied by 4.

At dilation scale 1, the curve C_1 corresponds to the curve C_0 dilated 3 times. New details appear since they are now bigger than unit δ (Fig. 1.C_1). The new measure of the curve is $\mu_\delta^1(C_1) = 4l_0$. At dilation scale 2, again, new details appear in C_2 leading to a length $\mu_\delta^1(C_2) = 16l_0$ (Fig. 1.C_2). At dilation scale n, the length of the curve measured with unit δ would be:

$$\mu_\delta^1(C_n) = 4^n\, l_0. \tag{8}$$

Now, let us consider the amount of space occupied by these objects. For the von Koch curve, we define the extension $\mathcal{E}(C_n)$ of C_n as the horizontal straight line encompassing the entire curve from left to right. The size of the extension, $\mu^1(\mathcal{E}(C_n))$ is thus simply the diameter of the curve. At the different dilation scales, we have $\mu^1(\mathcal{E}(C_0)) = l_0$, $\mu^1(\mathcal{E}(C_1)) = 3l_0$, $\mu^1(\mathcal{E}(C_2)) = 9l_0$, ... , and more generally:

$$\mu^1(\mathcal{E}(C_n)) = 3^n l_0. \tag{9}$$

At dilation scale n, the object C is dilated by a factor $\lambda = 3^n$, and the relationship between the total length, $\mu^1_\delta(C_n)$ and the size of its extension, $\mu^1(\mathcal{E}(C_n))$, can be obtained by eliminating n in the two preceding Eqs.:

$$\mu^1_\delta(C_n) = \mu^1(\mathcal{E}(C_n))^{\frac{\text{Log } 4}{\text{Log } 3}}. \tag{10}$$

where the exponent $\frac{\text{Log } 4}{\text{Log } 3}$ is the curve fractal dimension. This Eq. expresses a direct relationship between the measure of C_n at scale δ, $\mu^1_\delta(C_n)$ (here the length at scale δ) and the measure of its extension (reflecting the space occupation of the object). The actual length of the object at scale δ grows quicker than that of its extension throughout successive dilations. Note that, in a dual perspective, successive contractions of the measurement unit δ (δ_0=$l_0/2$ at scale 0, δ_1=$l_0/6$ at scale 1, $\delta_n = 1/(2.3^n)$ at scale n) would lead exactly to the same relationship.

Example 2. Let us consider a second theoretical example, closer to plant applications (Fig. 2). A plant-like object is generated recursively with a slightly modified iterated function system (IFS) (e.g. [13]). The initial object is a leaf, represented as a small horizontal disk (Fig. 2.a). At the first iteration step, the initial object P_0 is scaled by the IFS by a factor $s = 1/3$ and this contracted leaf is duplicated $k = 5$ times as indicated on Fig. 2.b. In addition to these classical transformation of an IFS, the result is then dilated by a factor 3 to keep the size of a leaf unchanged between two iteration steps, leading thus to object P_2 (Fig. 2.b). This process is then iterated using, at each step n, the object P_{n-1} resulting from the previous step as the initial object (Figs. 2.c and d). Note that the object obtained after the n-th iteration is scaled by a factor 3^n compared to the output of a classical IFS (*i.e.* without the dilation step). Up to this scaling factor, both objects have exactly the same spatial distribution of leaves and identical scaling structure. They both approach the theoretical self-similar dimension D_s as n increases:

$$D_s = \frac{\text{Log } k}{\text{Log } 1/s} = \frac{\text{Log } 5}{\text{Log } 3} = 1.465 \tag{11}$$

Figure 2. Theoretical plant canopies generated at the consecutive iteration steps of an IFS. After each iteration step n, the result is dilated by a factor 3^n to keep the size of a leaf constant.

For each iteration step of the modified IFS, the total leaf area $\mu^2_\delta(P_n)$ is:

$$\mu^2_\delta(P_n) = l\, k^n \tag{12}$$

where l is the surface of a leaf (proportional to δ^2).

For each theoretical plant P_n, an extension represented by a convex envelop $\mathcal{E}(P_n)$ can be computed (Fig. 3). The total surface of $\mathcal{E}(P_n)$, $\mu^2(\mathcal{E}(P_n))$, may be estimated numerically (see Sec. 3).

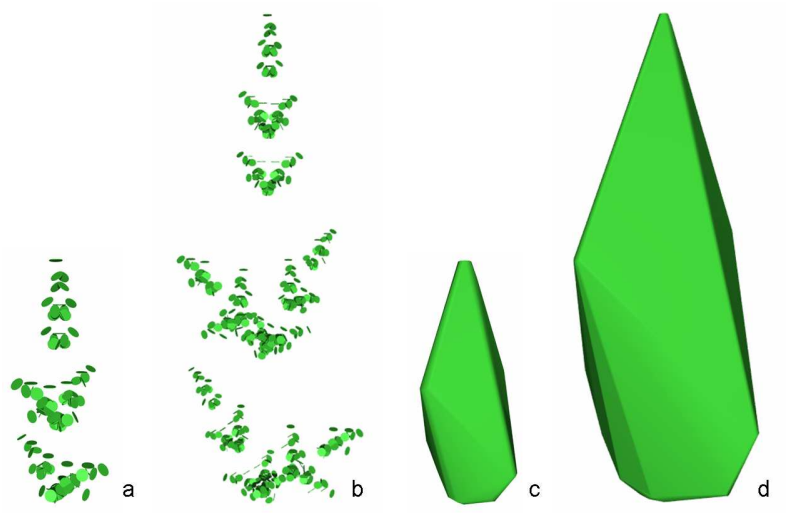

Figure 3. a. original leaf distribution. b. original distribution scaled by a factor s. c. envelop of the original distribution of leaves. d. Envelop scaled by a factor s.

The measures of both surfaces, the leaf and the envelop surface, can be compared by plotting $\mathrm{Log}(\mu^2_\delta(P_n))$ versus $\mathrm{Log}(\mu^2(\mathcal{E}(P_n)))$ for different values of the scaling factor s (Fig. 4). As indicated by Eq. (7), the slope α of this graph characterizes the fractal dimension of the object:

$$\tilde{D}_s = 2\alpha = 1.4786 \tag{13}$$

which is close to the theoretical value $D_s = 1.465$.

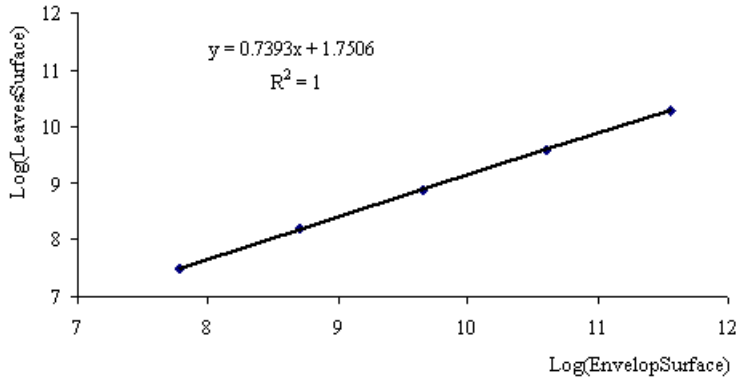

Figure 4. Log-Log regression between the envelop surface and the leaf surface of a series of theoretical canopies.

3 COMPUTING THE FRACTAL DIMENSION OF A PLANT USING ITS MULTISCALE ORGANIZATION AND THE TWO SURFACE METHOD

The two-surface method can be used to estimate the fractal dimension of real plant populations [10]. The method consists of comparing the total leaf area of each plant with the area of its crown envelop. If this comparison is made for a high enough number of individuals with varying sizes, a Log-Log regression between the two variables gives an estimate of d/D' (Eq. (7)). As proposed by Zeide and Pfeifer, the method can be applied on a collection of plant individuals with sufficient size variability. In this case, the estimated fractal dimension characterizes the geometry of an "average" plant corresponding to the class of all the individuals used in the estimation process. In this paper, we show how the two-surface method can be used to estimate the fractal dimension of a single individual.

Plants appear as intricate organisms due to the existence of numerous components of different types, called *modules,* in their structure [14], [15], [16]. At a particular level of organization, or *scale*, each individual plant can be decomposed into a set of modules of the same type, thus defining a particular *plant modularity* [17]. From finer to coarser scales, classical module types are metamers (nodes plus their internodes and their leaves), annual shoots (parts of a plant grown by a meristem during one year), axes (parts of a plant grown by a single bud), branches (branching systems grown by a bud and its descendants) or reiterated complexes (duplications of an adult plant borne by the plant itself). Plant modules are usually nested [17]. Modules from a coarser scale are composed of modules of finer scales, *e.g.* branches are composed of annual shoots and annual shoots are composed of metamers.

Within a given plant modularity, modules may bear leaves or not. *Leafy modules* are always located at the topological periphery of the plant due to the characteristic way plants grow: i) the young leaves are systematically added on new shoots; ii) the new shoots are themselves added at the periphery of the existing structure, which is thus itself not modified by this addition; iii) older leaves may fall out, which may thus result in an absence of leaves in the inner modules of the plant.

The possibility to apply the two surface method to a single plant stems from the following remark. Throughout the plant, leafy modules form a collection of branching systems with varying sizes. If the plant has a fractal nature, the relationship between the module size and their leaf area should respect Eq. (7).

To test this hypothesis, we designed an adapted methodology, which consists of the following steps.

Creating 3D representation of plants. Depending on the application, 3D plant representation can be either obtained by simulations based on theoretical models [18], [19] or by 3D digitizing of real plants [20] and [21]. 3D digitizing consists in simultaneously recording tree geometry, *i.e.* the spatial location of tree components, and tree topology, *i.e.* the physical connections between tree components. Spatial co-ordinates can be recorded by using an electromagnetic 3D digitizer [22] while tree topology can be described as a multiscale tree graph [17]. The latter allows the tree decomposition into components defined at several scales, and describes connections between tree components in terms of succession and branching.

Building multiscale representations. In the digitized plants, the finest modularity (*e.g.* the metamer scale) is represented by a directed tree graph $g = (V, E)$, where V is a set of vertices representing the plant components and E is a set of edges representing the adjacency between pairs of components (Fig. 5.a). We denote r the root vertex of g, *i.e.* the only vertex that has no parent vertex. If a directed path connects vertex v to vertex v' in the tree graph g, v' is called a descendant of v and we write: $v \leqslant v'$. Note that relation $\leqslant$ is a partial order relation on V. Given a vertex v of V, the sub-tree of g, rooted in v, and containing all the descendants of v in g, is called the *complete subtree of* v.

A *cut* C in a tree-graph is a set of vertices of V such that *i*) none of them is an ancestor of an other vertex in C, and *ii*) any terminal vertex (i.e. vertex with no descendant) in the tree graph is the descendant of a vertex from the cut (Fig. 5.b). We say that a cut C is greater than a cut C', if for any comparable vertices $v \in C$ and $v' \in C'$, $v' \leqslant v$ and we write $C' \leqslant C$. Given a

cut C, the *cut-forest* $f(C)$ of g is the set of complete subtrees of g such that the set of roots of $f(C)$ is C. Note that if a cut C' is greater than a cut C, then each tree of $f(C)$ contains a tree in $f(C')$.

In our approach, cuts are used to define the roots of the leafy modules. The resulting forest is thus a partition of the plant leaves into leafy modules. To define plant representations at different scales, a set of cut-forests is defined by an ordered series of cuts in the tree-graph g. These cut-forests are nested and define leafy modules at different scales with different types and sizes (Figs. 5.b and c). The cuts can be defined based on either a biological or an artificial criterion. Biological cuts would correspond to modules having a botanical basis, such as shoots or axes. Artificial cuts would correspond to all other types of definitions, such as modules having a main stem with a fixed length or a given number of metamers.

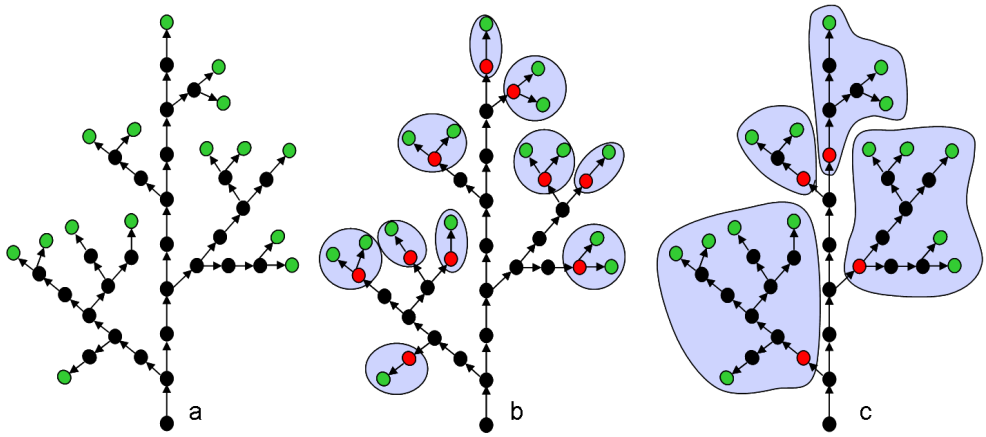

Figure 5. Definition of different types of leafy modules using different cuts. (a) tree-graph representing the plant topology at the finest scale. Leaf vertices are represented in green. (b) a fine-grain cut C' (vertices colored in red) defining small leafy modules. (c) a coarser cut C ($C \leqslant C'$) defining bigger groups of leaves.

Computing convex envelops. Each cut forest defines a set of complete subtrees corresponding to leafy modules. In the 3D space, each leafy module is represented by a set of geometric models representing its leaves. The convex envelop of this set is computed using the QuickHull algorithm [23].

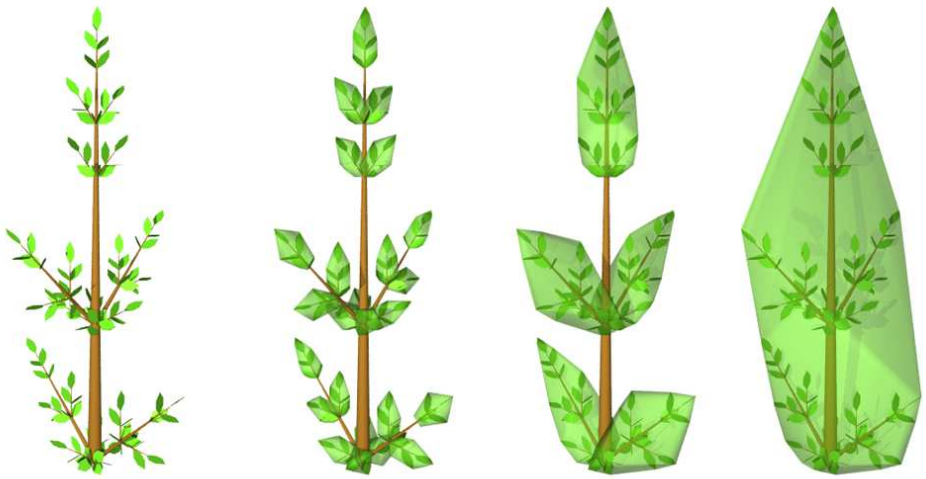

Figure 6. Leafy modules at different scales in a theoretical tree (a). Leafy modules are defined here by biological cuts corresponding to branching order 2 (b), 1 (c) and 0 (d). Their convex envelop were computed emphasizing how the overall plant geometry depends scale.

Figure 6 illustrates the result of these different steps on a theoretical tree. The plant geometry is first generated in 3D (Fig. 6.a). Then, different types of leafy modules are defined at different scales, here corresponding to different branching orders. This is carried out by identifying a totally ordered set of cuts in the original tree-graph corresponding to the different branching orders. Convex envelops of these modules are then computed at different scales (Figs. 6.b-d).

The fractal dimension of the plant can then be estimated from the Log-Log relationship between the surface of the convex envelop and the leaf area of each module. In addition, if the modules at a particular scale are sufficiently numerous and have varying lengths (which is not the case on this theoretical example), a fractal dimension can be computed more locally for the modules at this scale. The resulting dimension coefficients characterize the fractal nature of the plant at the considered scales. These coefficients need not be *a priori* identical. High variations would indicate a complex dependence of the structure upon scale, while weak variations would reflect a self-similar organization of the structure.

4 PEACH TREE FRACTAL DIMENSION

4.1 Plant Material

Four four-year peach trees (cv. August Red) were digitized in May 2001 in CTIFL Center, Nîmes, South of France, at shoot scale, one month after bud break. Plant digitizing made use of software 3A [24], which allows simultaneous recording of plant topology and geometry. Plant geometry was recorded using a magnetic digitizing device 3SPACE Fastrak [22], which records the coordinates of a pointer located on the plant organs. As described in [20], plant digitizing started at plant collar, i.e. the base of the trunk and each shoot was then described as a set of segments to take into account curvature and branching points. The resulting dataset was a multiscale tree graph (MTG, [17]) including both multiscale topology and spatial co-ordinates of organs ($\sim$3.700 co-ordinates per tree).

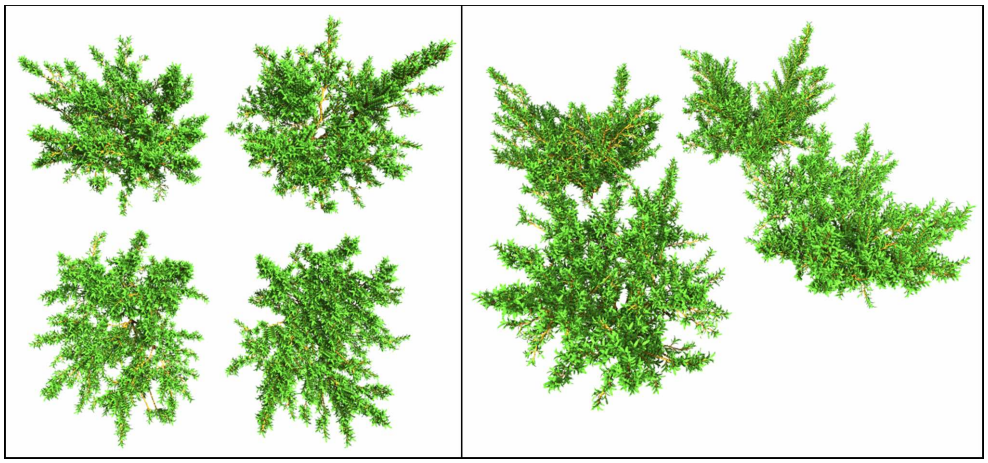

Figure 7. Four peach trees whose wood structures have been digitized. The geometry of the branches and the leaves have been reconstructed using AMAPmod [25]. The mock up have been rendered with Pov-Ray [26].

Different types of leafy modules were considered in the measurement protocols (Fig. 8.a) :

- *Current Year Shoots (CYS).* Wood structure of the current year that carry leaves. These plants are made up of several types of current year shoots:
    - Long shoots borne by one-year-old wood.

- Spurs, which are short shoots borne by one-year-old wood.
- Suckers, corresponding to vigorous branches borne by more than one-year-old wood.

- *One-Year-Old Shoots (OYOS)*. They correspond to the fruiting units managed by the peach tree growers.
- *Scaffolds*. They correspond to the main branching systems borne by the short trunk of the trees.
- *Crowns*. Whole leafy structure of the tree.

The origin vertices of these leafy modules were marked in the tree graphs representing each peach tree topology in order to retrieve all these botanically-defined leafy modules in subsequent treatments.

Given the high number of leaves ($\sim 15,000$ per tree), digitizing all leaves was impossible. Leaves attached to CYS were therefore reconstructed from a set of empirical rules [27] (Fig. 8.b). For this purpose, an additional set of thirty randomly sampled CYS (ten in each category - suckers; spurs and long shoots) were digitized at leaf level in order to assess the spatial distribution of leaves in CYS. The number of leaves and the average area of a CYS were estimated from an allometric relationship with CYS length, which was established for each shoot type. All leaves attached to a CYS were affected the same leaf area.

Allometric relationships for leaf length and leaf width as a function of leaf area were derived for each shoot type from the set of 30 digitized CYS at leaf scale. They were used to calibrate leaf shape to make leaves obey allometry laws between area and dimensions [28]. Internode lengths were assumed to be constant, so that leaf insertion points were regularly spaced along the shoot segment according to leaf rank. Finally, leaves orientation angles with respect to their bearing stem were assessed using distribution estimated from sampling.

The reconstruction of the virtual 3D representation of the tree was made using AMAPmod, an open software for plant architecture modelling, [25] (Fig. 7). Envelop-based multiscale representations of the trees were then constructed using the method described in Sec. 3 on the marked leafy modules (Figs. 8.c-d).

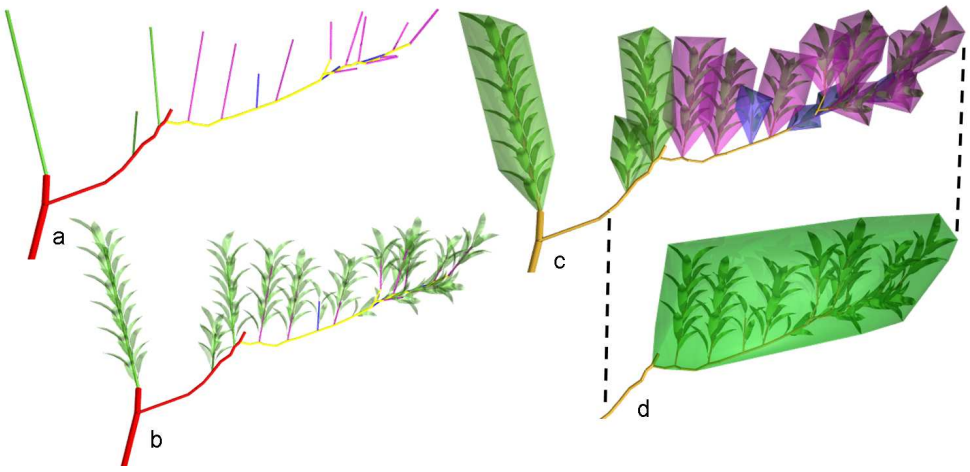

Figure 8. Structure of the peachtrees: (a) Digitized wood segments with different botanical types represented by colors : red for old wood, yellow for one-year-old shoot, green for the suckers, purple for the long shoots and blue for the short shoots. (b) 3D reconstruction of foliage using allometric relations between the length of shoots and their total leaf area. Construction of convex envelops corresponding to leafy modules defined by the (c) current year shoots, or (d) one-year-old shoots.

The multiscale structure of the peach trees is illustrated in Fig. 9 which shows volumic representations at the different scales, *i.e.* corresponding for each tree to a set of ordered cuts defined by the different types of leafy modules. The use of colors allows us to visualize the distribution of different types of elements at the same scale. On the top left picture, the short shoots are represented in blue, the long shoots in purple and the suckers in green. The suckers are located in the center of the crown while the two others types are distributed in the periphery. The spatial distribution of the different branching systems and their entanglement can be visually appreciated on these representations. For instance in the bottom left picture of Fig. 9, scaffolds appear regularly distributed in the crowns except for the first tree, where entangled systems can be observed.

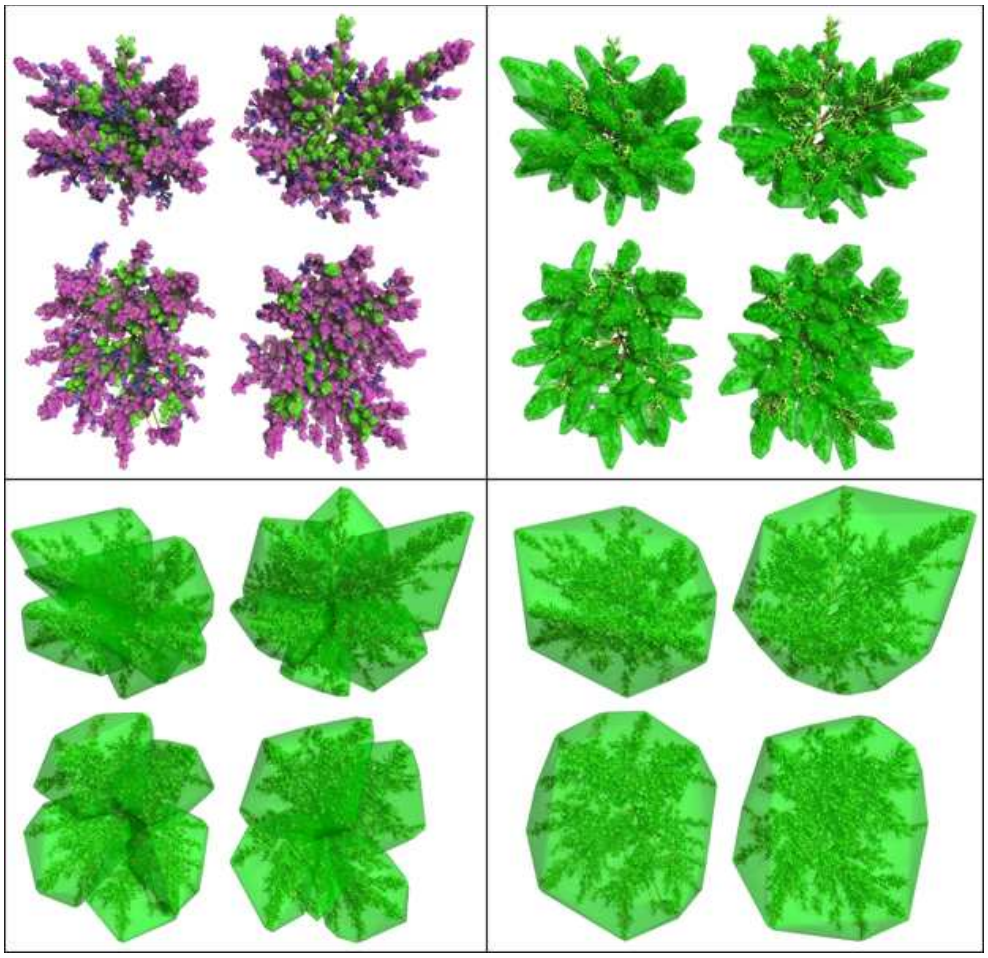

Figure 9. Multiscale representation of the peachtrees. From left to right and top to bottom, representations of the leafy modules at the scale of current year shoots, one-year-old shoots, scaffolds and crowns. In the first picture, three colors are used to make the difference between short shoots (blue), long shoots (purple) from suckers (green).

Different characteristics were computed for the different types of leafy modules to charac-

terize them (Tab. 1). The number of elements grows exponentially at increasingly finer scales (this variation is studied more precisely in Sec. 4.3). Leaf area density (i.e. ratio of leaf area to envelop volume of any leafy module) is stable at the coarsest scales, then increases rapidly.

	Crowns		Scaffolds		OYOS		CYS		Leaves	
	Mean	s.d.	Mean	s.d.	Mean	s.d.	Mean	s.d.	Mean	s.d.
Nb Elements	1	0	5	0.8	99	8.9	1765	247.1	14705	823.4
Element Surface (m^2)	29.15	2.76	8.97	2.58	0.57	0.37	0.0585	0.0572	0.002	0.0005
Element Volume (m^3)	13.09	1.89	2.14	0.96	0.036	0.034	0.0012	0.0019		
Leaf Area Density	2.32	0.26	2.93	0.84	9.55	4.26	18.06	2.47		

Table 1. Number of elements per tree at the different scales, with their mean surfaces (m^2), mean volumes (m^3) and leaf area density (m^2/m^3).

The scale of the leafy modules can be further characterized by comparing their surfaces (Fig. 10). Each level of organization contains elements with surfaces included in a certain range. On Fig. 10.a, the histogram of the leafy module surfaces per scale provides an estimate of the range of surfaces in each level of organization. Two main classes of leaf surface can be observed, corresponding to the two classes of shoots, *i.e.* long and short, which have different allometric relationships for leaf area reconstruction. A peak also appears in the CYS curve which correspond to a small variability of the short CYS. Figure 10.b shows the total leafy module area at the different scales. The more detailed the representation, the larger the surface. However, at leaf scale a decrease of the total area is observed due to a difference in nature of the origin of the considered surfaces: envelops essentially represent how the plant branching structures colonize space and are roughly independent of the leaf size, while leaf surfaces are independent of the plant branching strategy.

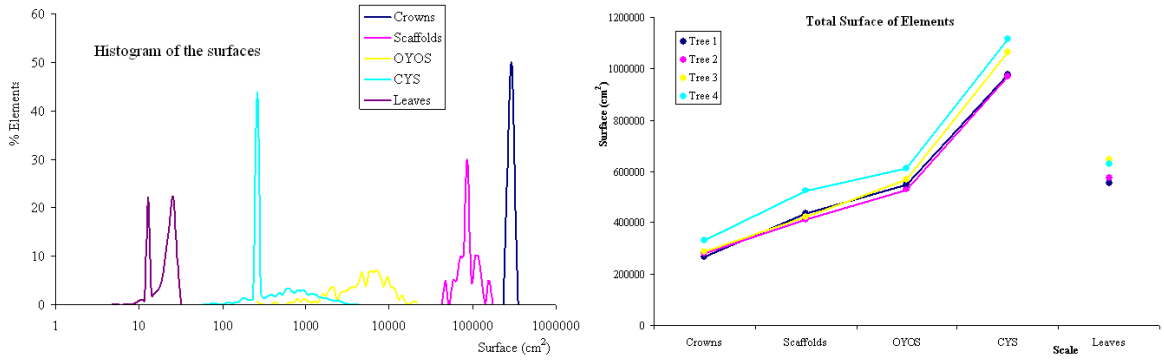

Figure 10. Left: Histogram of the leafy module surfaces per levels of organization. Right: Total surface of the leafy modules as a function of scale.

4.2 Estimating the Fractal Dimensions of Tree Crowns

All leafy modules at all scales were considered and the respective areas of their convex envelop E and leaf content L were computed. According to Eq. (7), if the tree crowns are fractal, there must be an allometric relationship between these two quantities of the form:

$$L = aE^{d/2} \tag{14}$$

Figure 11 shows the Log-Log diagrams between the leaf and the convex envelop areas of peach

tree module for each individual tree. The slope of the regression gives us the values $\frac{d}{2}$. All the points, computed from the branching systems at different biological scales and structural complexities, are aligned within each category of leafy modules (at CYS, OYOS and scaffold scales respectively) and between these categories showing a marked self-similarity among scales. Corresponding fractal dimensions estimated for the 4 peach trees are very stable (between 2.33 and 2.38), with an overall regression coefficient greater than 0.97, each slope coefficient being significant at 0.05 level (Tab. 2, all scales).

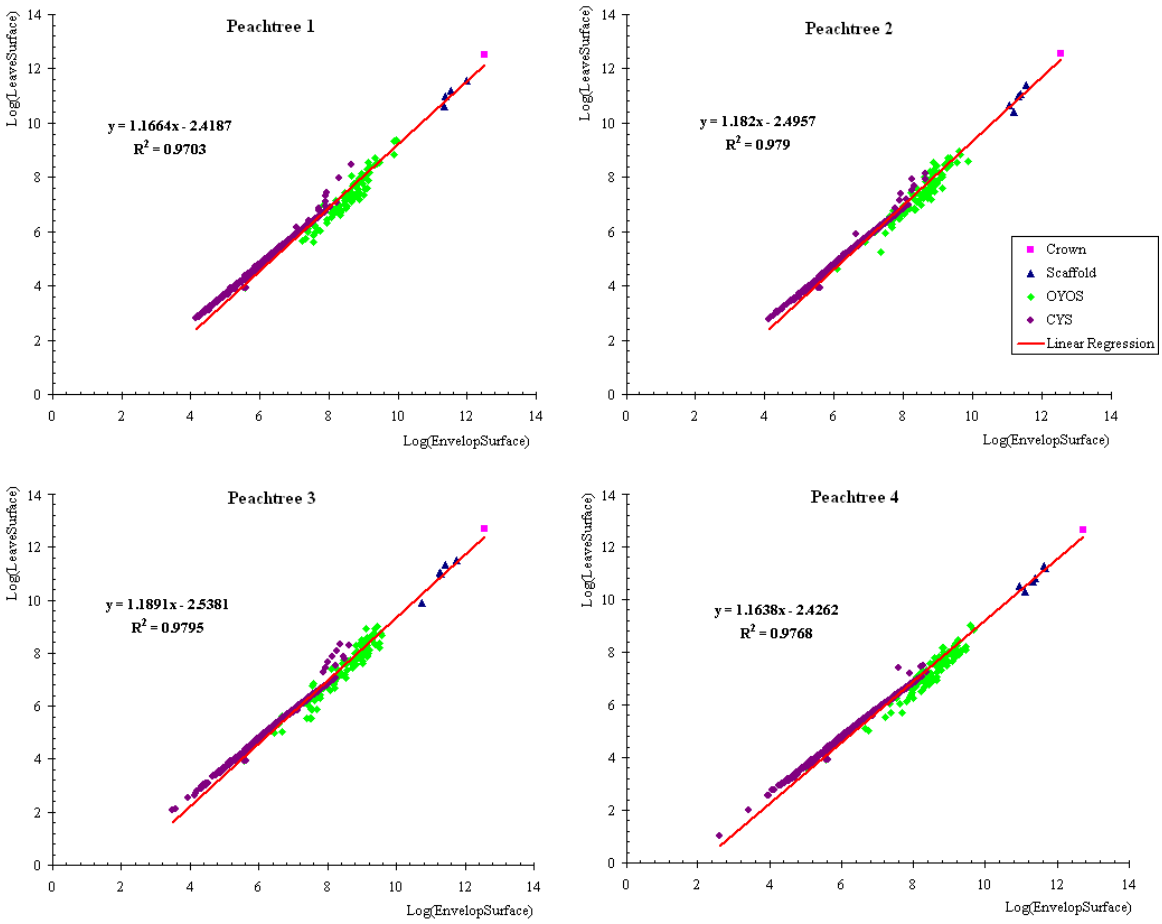

Figure 11. Linear regression between the log of the convex envelops surfaces and the log of the leaves surfaces. All branching systems (leafy modules) at all scales are considered.

At individual scales, it is possible to consider partial regressions, restricted to branching systems of a particular type (instead of merging all branching systems at all scales). Due to the size variation of the modules at each particular scale, the two surface method can still be applied "locally". The resulting fractal dimension can be interpreted as a "local dimension", reflecting the self-similarity of the leafy modules around the considered scale (Tab. 2). If the plant is self-similar, all these "local dimensions" will tend to be identical. In the opposite case, these different coefficients express a change in the structure of the plant as a function of scale. In the peach trees, we observe very close values at CYS, OYOS scales and when all scales are considered together (2.38 ± 0.9), thus confirming the marked self-similar organization of the peach tree foliage. An exception to this constant scaling variation appears at the scaffolds scale

when all trees are considered. At this scale, the local dimension is slightly higher (2.77) and reflects a locally more dense occupation of space at the scaffolds scale.

We must note in this method that the current year shoots are linear compounds whose leaves shapes and numbers are determined with allometric relationships depending of their lengths. Because of this reconstruction process, the convex envelop surface and leaves area of these small branching systems are highly correlated. This artefact of the reconstruction method influences mainly the bottom part of the point clouds, leading to linear point sets. Other branching systems than current year shoots have more irregular branching structure, leading to greater variability in the point clouds.

	Peachtree 1		Peachtree 2		Peachtree 3		Peachtree 4		All	
	d	r^2	d	r^2	d	r^2	d	r^2	d	r^2
CYS	2.44	0.96	2.44	0.97	2.42	0.97	2.42	0.97	2.44	0.97
OYOS	2.47	0.91	2.30	0.92	2.44	0.94	2.29	0.93	2.35	0.92
Scaffolds	n.s.		n.s.		n.s.		n.s.		2.77	0.82
All scales	2.33	0.97	2.36	0.98	2.38	0.97	2.33	0.98	2.35	0.97

Table 2. Fractal dimension of the different trees computed for all types of branching systems and more locally for each type of branching system (CYS, OYOS and Scaffolds). The low number of scaffolds of individual trees does not allow to compute significant regression coefficients. However, these coefficients can be computed when all tree branching systems are merged together.

4.3 Comparison with the Box-Counting Method

We compared the two-surface with the box-counting method as a reference method which has been extensively used to estimate fractal dimension of objects embedded in the plane. For this purpose, we adapted the box-counting method to 3-D analysis by building 3-D grids dividing space into voxels of size δ and detecting intersection of 3-D objects with grids of varying voxel size. 3-D objects consisted of triangular meshes and detection of intersections with the voxel grid was carried out using the algorithm described in [29]. If $N(\delta)$ denotes the number of intercepted voxels of size δ the box-counting estimator of the fractal dimension D_δ of the object is defined as:

$$D_\delta = \lim_{\delta \to 0} \frac{\ln N(\delta)}{\ln \frac{1}{\delta}} \tag{15}$$

In practice, only a finite range of scales are considered between $\delta_{\min}$ and $\delta_{\max}$ [4]. $\delta_{\min}$ is chosen of the order of magnitude of a plant leaf, while $\delta_{\max}$ typically corresponds to the size of the plant bounding box. Several grid shifts and rotations were tested with respect to the plant and grids corresponding to the minimum number of intercepted boxes were considered for the fractal dimension estimation. Results of this method on the different peachtrees are given in Tab. 3. These results are very close to the estimates provided by the two surface method (Tab. 2, the maximum difference between the two estimated fractal coefficients being less than 0.04). Both methods thus give consistent results.

Peachtree 1	Peachtree 2	Peachtree 3	Peachtree 4
2.37	2.39	2.36	2.36

Table 3. Fractal dimension of the peachtrees computed using the Box-Counting method.

Interestingly, the developed methodology made it possible to compute the fractal dimension of peach trees using a variant of the box-counting method, where boxes correspond to foliage envelops. Indeed, the computed envelops at the different scales represent different covers of the plant foliage at different scales. Let us denote δ the average diameter of envelops at a given scale (resp. CYS, OYOS, Scaffold and Crowns) and $N(\delta)$ the number of envelops at this scale. In practice, δ is estimated as the square root of the average envelop surface at each scale (Tab. 1 Element Surface). The fractal dimension of the plant can thus be estimated by Eq. (15) as well [12]. We tested this estimation method with the envelops computed for the two-surface method.

Results are presented in Fig. 12. Estimated fractal dimensions between 2.36 and 2.39 are in very good accordance with both the classical box-counting method and with the two surface method.

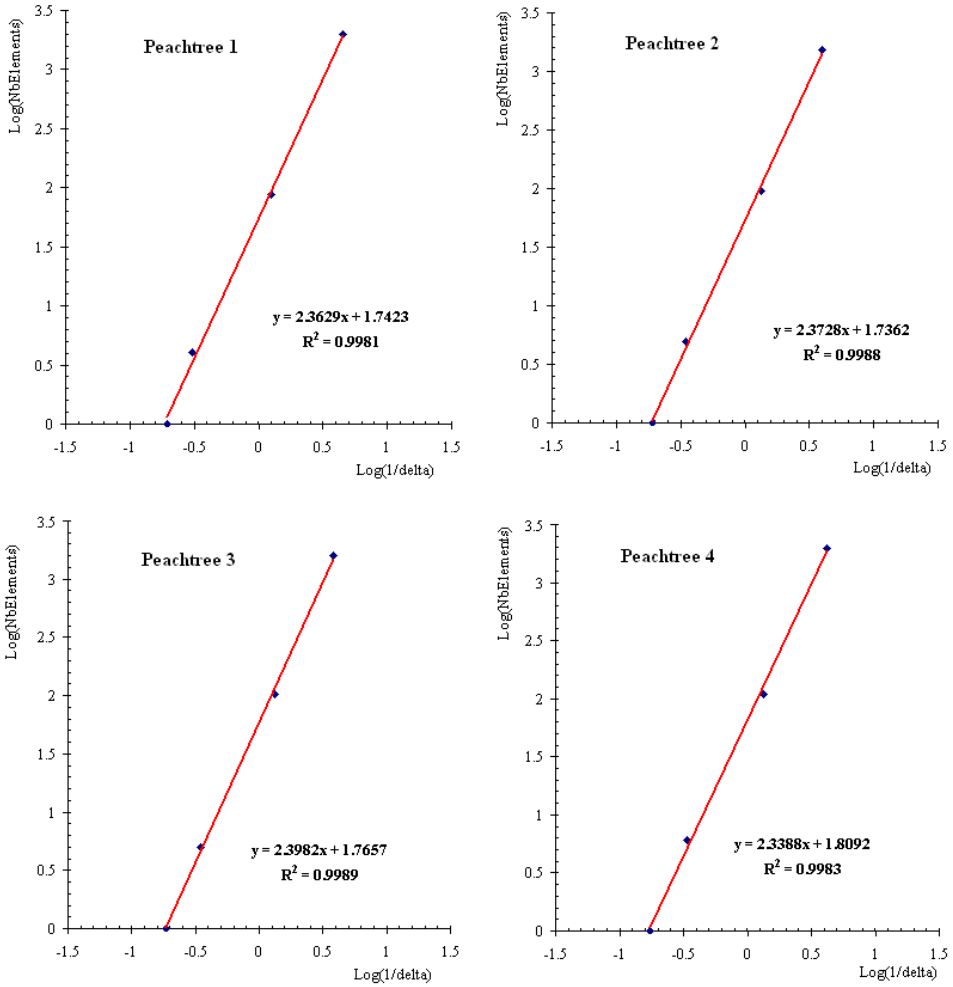

Figure 12. Variant of the box counting method using envelops computed in the two-surface method as boxes. Log-Log diagrams between $N(\delta)$ and $1/\delta$ are shown for the 4 peach trees. Estimated fractal dimensions are comprised between 2.36 and 2.39.

5 CONCLUSION

In this paper, we presented a method derived from the two-surface method to estimate the fractal dimension of plant foliage. This method consists of i) digitizing in 3D the plant topology and geometry, ii) extracting different types of leafy modules of different sizes from the plant database, using the topological information iii) comparing the total leaf area and the convex envelop area of these leafy modules which is computed from the digitized geometric information. The method was applied to a set of 4 digitized peach trees and gave similar estimates of the fractal dimension for the 4 trees. We also estimated the fractal dimension of the same trees using the classical box-counting method adapted to 3D-geometry, and a variant of this method based on envelops, which both gave results consistent with our method. In addition to an overall fractal dimension coefficient, the method enabled us to estimate "local dimensions", i.e. fractal dimension coefficients that correspond to particular types of plant components at different levels of organization. Such coefficients make it possible to characterize the variation of the fractal nature of the plant throughout scales. They could be of much value in the botanic analysis of

plant architecture and ecophysiological models. This work suggests that methods based on envelop computing are applicable to plant architecture analysis. In particular, they can overcome limitations of classical method such as the lack of accuracy of the standard box counting method [30]. More generally, by exploiting the topological organization of plants at different scales, these envelop-based methods are adapted to explore the multiscale nature of plants.

Bibliography

[1] C. Godin and H. Sinoquet, New Phytologist **166**, 705 (2005).

[2] A. D. Bell, *Plant form. An illustrated guide to flowering plant morphology*, Oxford University Press, Oxford, 1991.

[3] P. M. Iannaccone and M. Khokha, editors, *Fractal geometry in biological systems: an analytical approach*, CRC Press, Bocan Raton, 1996.

[4] B. B. Mandelbrot, *The fractal geometry of nature*, W.N. Freeman, USA, 1983.

[5] A. H. Fitter, New Phytologist **106**, 61 (1987).

[6] A. Eshel, Plant, Cell and Environment **21**, 247 (1998).

[7] A. L. Oppelt, W. Kurth, H. Dzierzon, G. Jentschke, and D. L. GodBold, Annals of Forest Science **57**, 463 (2000).

[8] D. Morse, J. Lawton, M. Dodson, and M. Williamson, Nature **314**, 731 (1985).

[9] J. R. Castrejon Pita, A. Sarmiento Galan, and R. Castrejon Garcia, Fractals **10**, 429 (2002).

[10] B. Zeide and P. Pfeifer, Forest Science **37**, 1253 (1991).

[11] B. Zeide, Forest Ecology and Management **46**, 179 (1991).

[12] K. Falconer, *Fractal geometry: mathematical foundation and applications*, John Wiley and Sons, 1990.

[13] M. Barnsley, *Fractals everywhere*, Academic Press, Boston, 1988.

[14] J. L. Harper, B. R. Rosen, and J. White, *The growth and form of modular organisms*, The Royal Society, London, UK, 1986.

[15] D. Barthélémy, Y. Caraglio, and E. Costes, Architecture, gradients morphogénétiques et âge physiologique chez les végétaux, in *Modélisation et Simulation de l'Architecture des Végétaux*, edited by J. Bouchon, P. d. Reffye, and D. Barthélémy, Science Update, pages 89–136, INRA Editions, Paris, France, 1997.

[16] P. Room, L. Maillette, and J. Hanan, Advances in Ecological Research **25**, 105 (1994).

[17] C. Godin and Y. Caraglio, Journal of Theoretical Biology **191**, 1 (1998).

[18] P. Prusinkiewicz, Selfsimilarity in plants : integrating mathematical and biological perspectives., in *Thinking in Patterns: Fractals and Related Phenomena in Nature*, edited by M. M. Novak, pages 103–118, World Scientific, Singapore, 2004.

[19] P. Ferraro, C. Godin, and P. Prusinkiewicz, Fractals **13**, 91 (2005).

[20] H. Sinoquet and P. Rivet, Trees : Structure and Function **11**, 265 (1997).

[21] C. Godin, E. Costes, and H. Sinoquet, Annals of Botany **84**, 343 (1999).

[22] X. Polhemus, 3space fastrak users manual, revision f, Technical report, Polhemus Inc., 1993.

[23] C. B. Barber, D. P. Dobkin, and H. Huhdanpaa, ACM Transactions on Mathematical Software **22**, 469 (1996).

[24] B. Adam, H. Sinoquet, and C. Godin, 3a version 1.0 : Un logiciel pour l'acquisition de l'architecture des arbres, intégrant la saisie simultanée de la topologie au format AMAPmod et de la géomtérie par digitalisation 3d. guide de l'utilisateur, Technical report, INRA-PIAF, 1999.

[25] C. Godin et al., AMAPmod v1.8. introduction and reference manual, Manuel de logiciels, CIRAD, 1997-2002.

[26] POV-Ray, Persistence of vision raytracer, 1991–2003.

[27] G. Sonohat, H. Sinoquet, V. Kulandaivelu, D. Combes, and F. Lescourret, Tree Physiology (2005), in press.

[28] H. Sinoquet, S. Thanisawanyangkura, H. Mabrouk, and P. Kasemsap, Annals of Botany **82**, 203 (1998).

[29] E. Andres, P. Nehlig, and J. Francon, Supercover of straight lines, planes and triangles, in *DGCI '97: Proceedings of the 7th International Workshop on Discrete Geometry for Computer Imagery*, pages 243–254, London, UK, 1997, Springer-Verlag.

[30] C. Tricot, *Courbes et dimensions fractales*, Springer Verlag et Editions Sciences et Culture, Paris, France, 1993.